Electronic Supplementary Material (ESI) for Green Chemistry.

Supporting Information

Atomically dispersed Co^{2+} on $MgAlO_x$ boosting C_{4-10} alcohols selectivity of ethanol valorization

Wen-Lu Lv, [a] Lei He [a], Wen-Cui Li [a], Bai-Chuan Zhou [a], Shao-Pei Lv [a], and An-Hui Lu [a] *

State Key Laboratory of Fine Chemicals, Liaoning Key Laboratory for Catalytic Conversion of Carbon Resources, School of Chemical Engineering, Dalian University of Technology, Dalian 116024, P. R. China.

Contents

1. Experimental methods

1.1 Catalyst preparation

Mg_3AlO_x was synthesized by the coprecipitation method. Briefly, 50 mL cation solution containing $Mg(NO_3)_2 \cdot 6H_2O$, and $Al(NO_3)_3 \cdot 9H_2O$ (Mg/Al molar ratio=3) was added dropwise to 50 mL solution containing Na_2CO_3, and NaOH at a speed of 2.5 $mL \cdot min^{-1}$. Then, 3 $mol \cdot L^{-1}$ NaOH aqueous solution was added to the solution to adjust an initial system pH to 10. The slurry was stirred for 18 h at 338 K. After filtration, the hydrotalcite was washed with deionized water repeatedly, and then dried at 323 K overnight. Finally, the dry precursor was calcined at 873 K in air for 2 h with a temperature ramp of 5 $K \cdot min^{-1}$. The prepared catalyst was denoted by Mg_3AlO_x. $Co_{0.15}Mg_{2.85}AlO_x$ catalysts were also prepared by the coprecipitation method. The cation solution containing proportional $Mg(NO_3)_2 \cdot 6H_2O$, $Al(NO_3)_3 \cdot 9H_2O$, and $Co(NO_3)_2 \cdot 6H_2O$ was added dropwise to solution containing Na_2CO_3, and NaOH at the first step. The other steps are the same as described above. The actual Co content was determined by ICP-OES to be 4.8 wt.%. $Co_{0.15}Mg_{2.85}AlO_x$-IM was prepared by incipient wetness method. In brief, $Mg_{2.85}AlO_x$ was impregnated with an aqueous solution of $Co(NO_3)_2 \cdot 6H_2O$ to achieve incipient wetness and held at room temperature for 120 min. As-prepared catalyst was obtained by drying at 323 K in flowing air overnight and calcining at 623 K for 2 h in static air. The actual Co content was determined by ICP-OES to be 4.8 wt.%.

1.2 Characterization

Powder X-ray diffraction (XRD) patterns were obtained with a Panalytical X'pert Pro Super X-ray diffractometer using Cu Kα radiation (40 kV, 40 mA, λ =0.15418 nm). Transmission electron microscopy (TEM), high angle angular dark field-scanning transmission electron microscopy

(HAADF-STEM), and energy-dispersive X-ray spectroscopy (EDS) elemental mapping were performed using a Tecnai F30 high-resolution transmission electron microscope (FEI Company). The actual Co content of the catalysts was determined using an Optima 2000DV instrument by ICP-OES.

Temperature-programmed reduction under H_2 atmosphere (H_2-TPR) was carried out on a Micromeritics AutoChem II 2920 apparatus. Each 100 mg catalysts (40-60 meshes) were loaded into quartz U tubes, then heated in 8 vol% H_2/Ar at a heating rate of 10 °C/min up to 873 K. A thermal conductivity detector (TCD) was used to calculate the amount of hydrogen consumption during the experiment. The type and number of base and acid sites on various catalysts surfaces were determined by temperature programmed desorption mass spectrometry (TPD-MS) of CO_2 and NH_3, respectively, using a Micromeritics AutoChem II 2920 apparatus as well. Signals for CO_2 (m/z = 44) and NH_3 (m/z = 15) were monitored using on-line mass spectrometry (MS).

X-ray photoelectron spectroscopy (XPS) was performed with a PHI Versaprobe 5000 spectrometer equipped with an Al Kα X-ray source. Binding energies were calibrated using the C 1s signal at 284.8 eV. Before the experiments, the samples were pre-treated in 8% H_2/N_2 at 773 K for 2 h.

The UV–vis diffuse reflectance spectra (UV–vis DRS) were collected using $BaSO_4$ as a reference on an Agilent Cary 5000 UV–vis–NIR spectrophotometer with a diffuse reflectance integration sphere attachment (Internal DRA 2500). The scanning was performed in a wavelength range of 200-800 nm at room temperature for a sample loaded in a transparent quartz cell.

1.3 Catalytic tests

All experiments were performed in a quartz-tube, packed-bed reactor (8-mm i.d.) under atmospheric pressure. Before reaction, a 200 mg catalyst was pretreated at 673 K for 2 h using 8 vol% H_2 in N_2. The reaction temperature was maintained using a vertically aligned tube furnace equipped with a YuDian AI controller (series 708P) and a K-type thermocouple.

All experiments were carried out under atmospheric pressure with a total gas flow rate of 30 mL/min. A Gas Chromatograph (GC) with a Flame Ionization Detector (FID) was connected to the reactor outlet to analyze the products. The carbon balance was better than 98%. The retention time for each specific component was determined using the corresponding standard chemicals (C_2-C_{10} *n*-alcohols, Sinopharm; C_2, C_6, C_8 *n*-aldehydes, Aladdin; E-2-butenal, AcroSeal). The identities of products were further confirmed by GC-MS analysis (Agilent 7890A GC interfaced with 5975C MS).

The ethanol conversion and product selectivity (except H_2) were calculated based on moles of carbon in the products, as follows:

Ethanol conversion:

$$Con.(\%) = (1 - \frac{n_{\text{out},C2H5OH} \times A_{\text{out},C2H5OH} \times f_{\text{out},C2H5OH}}{n_{\text{out},C2H5OH} \times A_{out,C2H5OH} \times f_{out,C2H5OH} + \sum_{i\geq 2} n_i \times A_i \times f_i}) \times 100\% \quad (1)$$

Product selectivity:

$$Sel.(\%) = \frac{n_i \times A_i \times f_i}{\sum_{i\geq 2} n_i \times A_i \times f_i} \times 100\% \quad (2)$$

$$Sel.(\%)\ of\ H_2 = \frac{m_{H_2}}{\sum_{i\geq 1} m_i} \times 100\% \quad (3)$$

The carbon number, FID peak area, response factor, and molar yield of each product are designated n_i, A_i, f_i, and m_i, respectively.

2. Performance of ethanol on Mg_3AlO_x and $Co_{0.15}Mg_{2.85}AlO_x$ at different temperatures

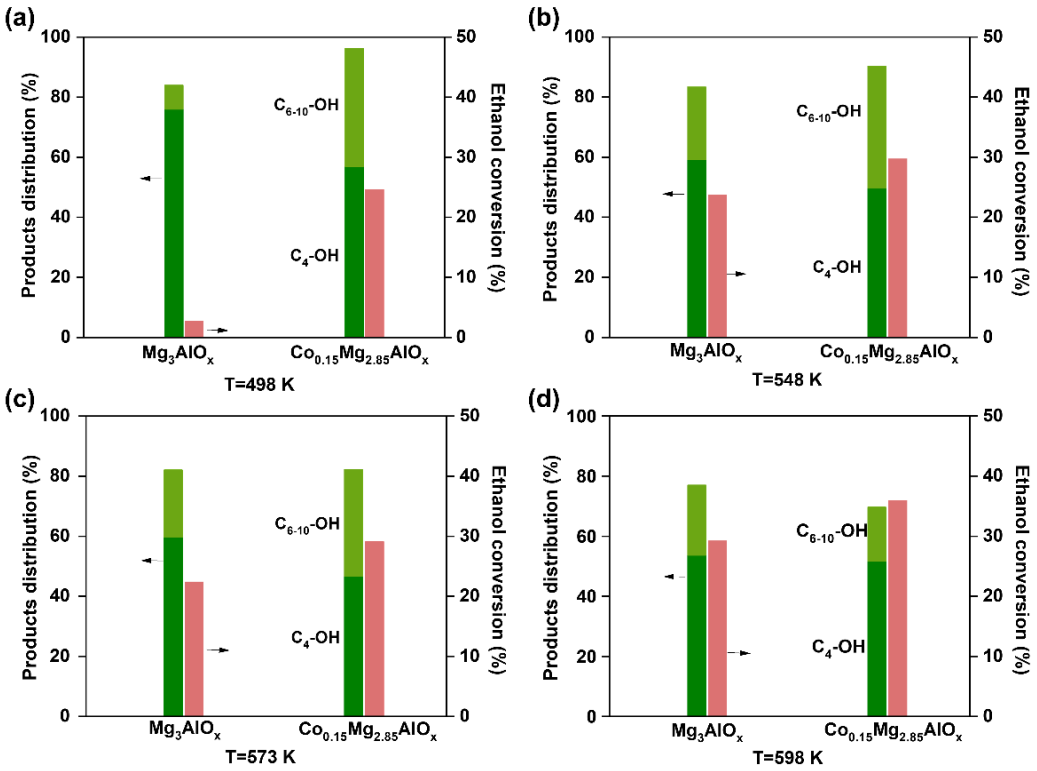

Figure S1. Comparison of ethanol conversion and product distribution over Mg_3AlO_x and $Co_{0.15}Mg_{2.85}AlO_x$ at 498 K (a), 548 K (b), 573 K (c), and 598 K (d). Reaction conditions: 0.2 g catalysts, 5.7 kPa C_2H_5OH, WHSV=0.96 g_{C2H5OH} $g_{Cat.}$ h^{-1}, V_{total}=30 mL/min, N_2 balance.

3. Performance of ethanol on Mg_3AlO_X, $Co_{0.15}Mg_{2.85}AlO_x$ and $Co_{0.15}Mg_{2.85}AlO_x$-IM at 523 K

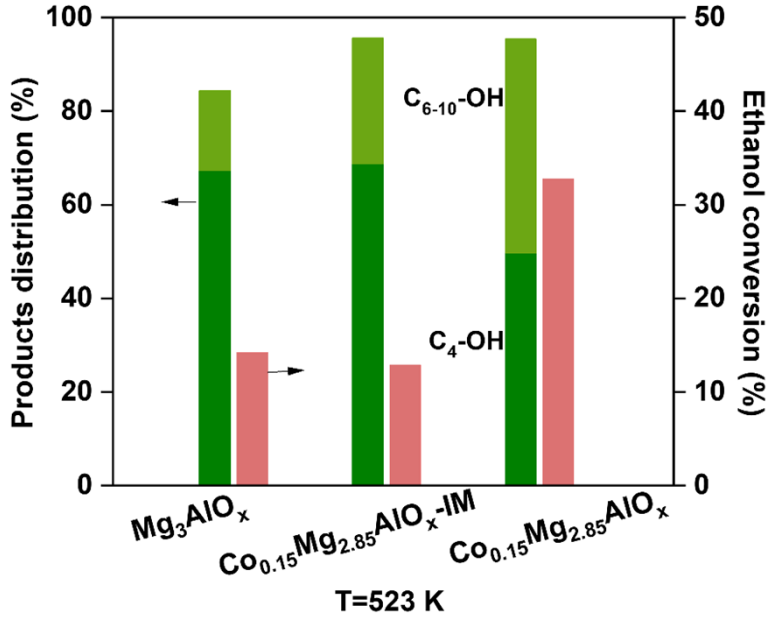

Figure S2. Comparison of ethanol conversion and product distribution over Mg_3AlO_x, $Co_{0.15}Mg_{2.85}AlO_x$ and $Co_{0.15}Mg_{2.85}AlO_x$-IM at 523 K. Reaction conditions: 0.2 g catalysts, 5.7 kPa C_2H_5OH, WHSV=0.96 g_{C2H5OH} $g_{Cat.}$ h^{-1}, V_{total}=30 mL/min, N_2 balance.

4. Performance of ethanol on $Co_{0.15}Mg_{2.85}AlO_x$ reduced at different temperatures

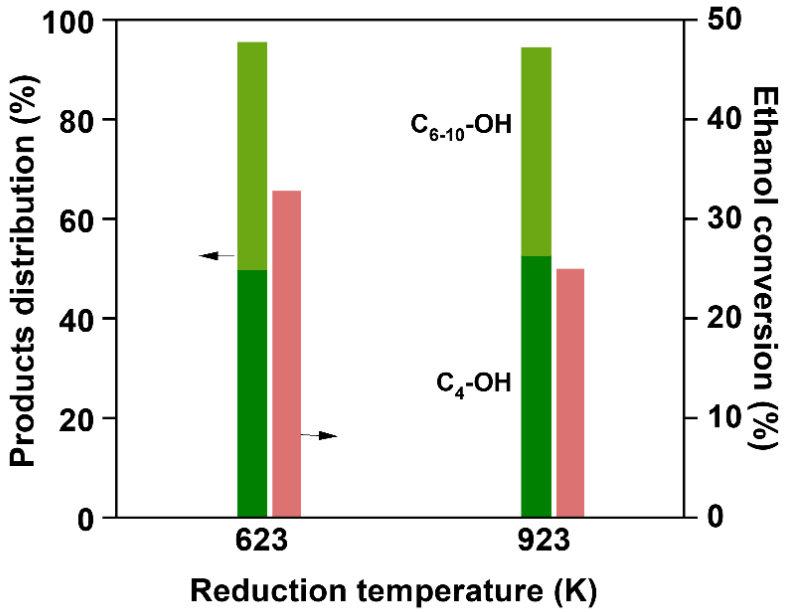

Figure S3. Comparison of ethanol conversion and product distribution over $Co_{0.15}Mg_{2.85}AlO_x$ reduced at different temperatures. Reaction conditions: 0.2 g catalysts, 5.7 kPa C_2H_5OH, WHSV=0.96 g_{C2H5OH} $g_{Cat.}$ h^{-1}, V_{total}=30 mL/min, N_2 balance.

5. TEM images of $Co_{0.15}Mg_{2.85}AlO_x$

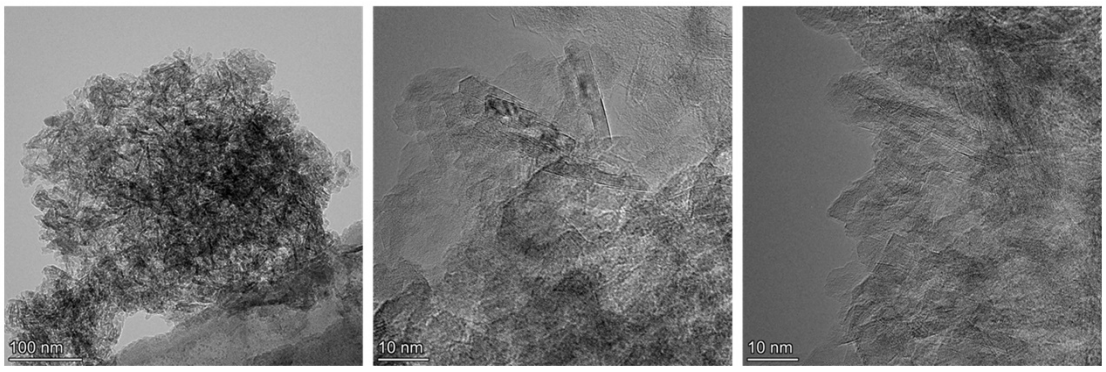

Figure S4. TEM images of $Co_{0.15}Mg_{2.85}AlO_x$ catalyst.

6. TEM images of used $Co_{0.15}Mg_{2.85}AlO_x$

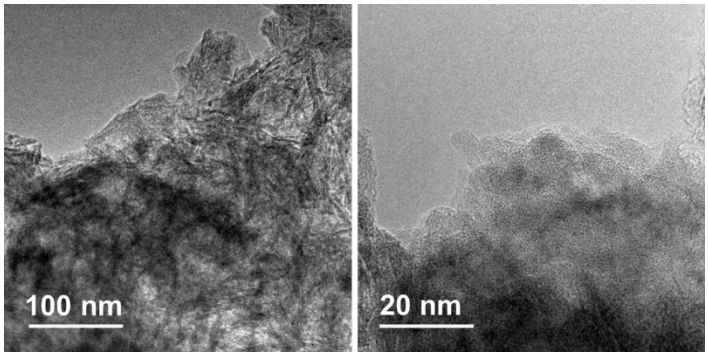

Figure S5. TEM images of used $Co_{0.15}Mg_{2.85}AlO_x$ catalyst.

7. XRD profiles of used $Co_nMg_{3-n}AlO_x$ catalysts

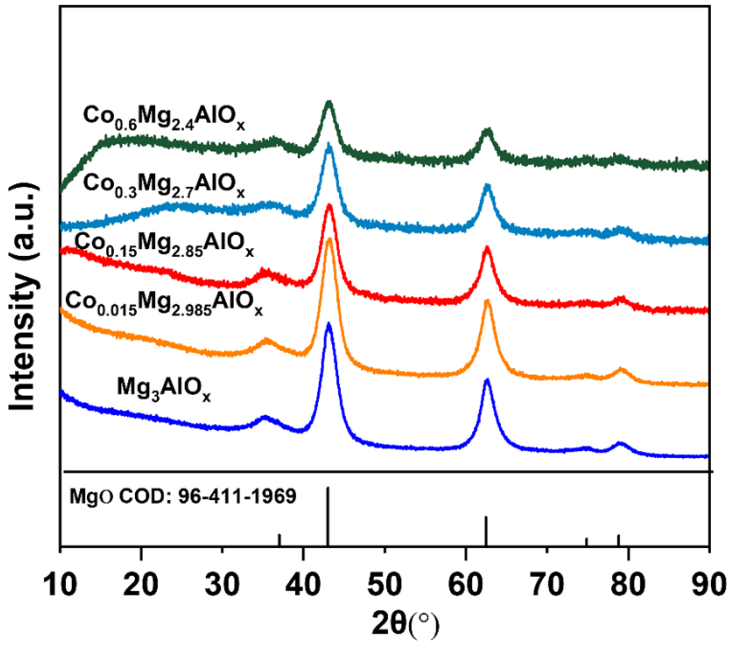

Figure S6. XRD profiles of $Co_nMg_{3-n}AlO_x$ catalysts after reaction.

8. XRD profiles of $Co_{0.15}Mg_{2.85}AlO_x$-IM

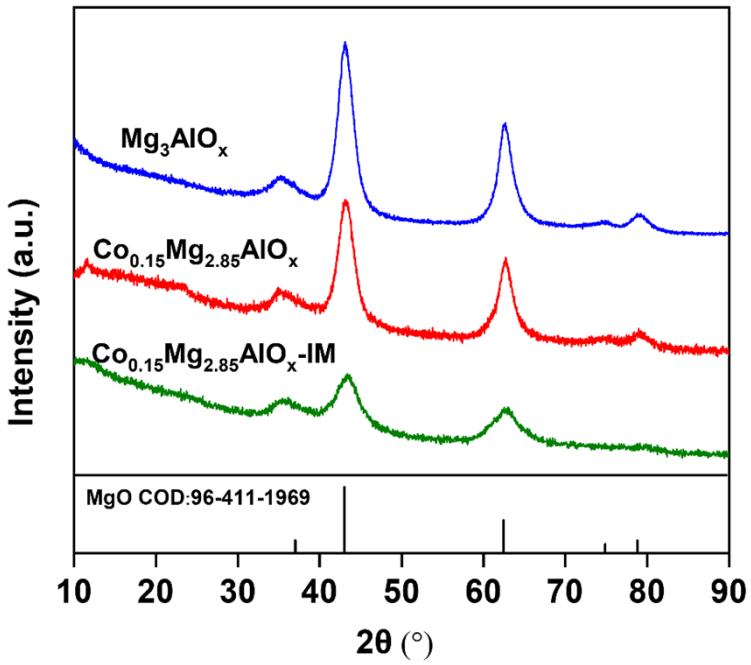

Figure S7. XRD profiles of Mg_3AlO_x, $Co_{0.15}Mg_{2.85}AlO_x$ and $Co_{0.15}Mg_{2.85}AlO_x$-IM catalysts.

9. XP spectra of Mg_3AlO_x and $Co_{0.15}Mg_{2.85}AlO_x$

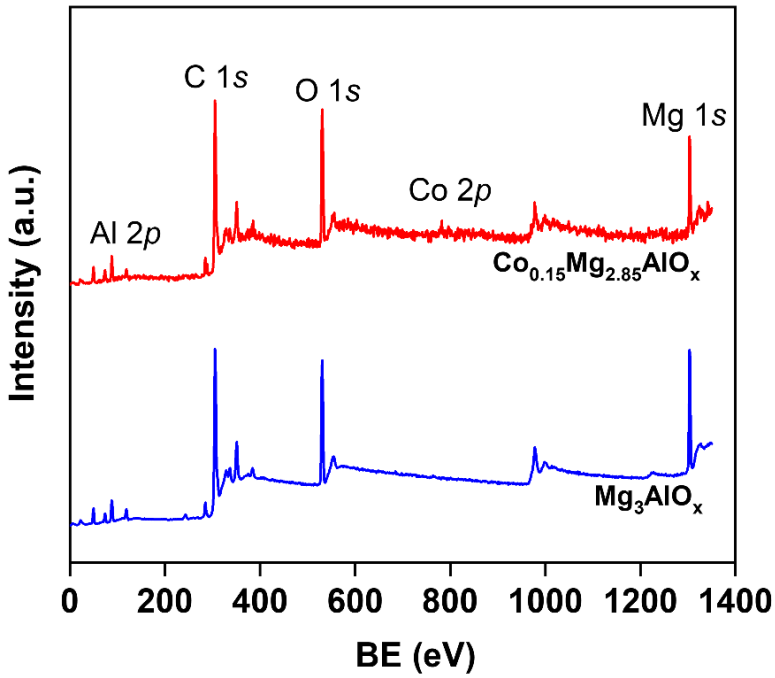

Figure S8. Full-range scan of XP spectra for Mg_3AlO_x and $Co_{0.15}Mg_{2.85}AlO_x$

10. Co 2*p* and O 1*s* XP spectra for $Co_nMg_{3-n}AlO_x$

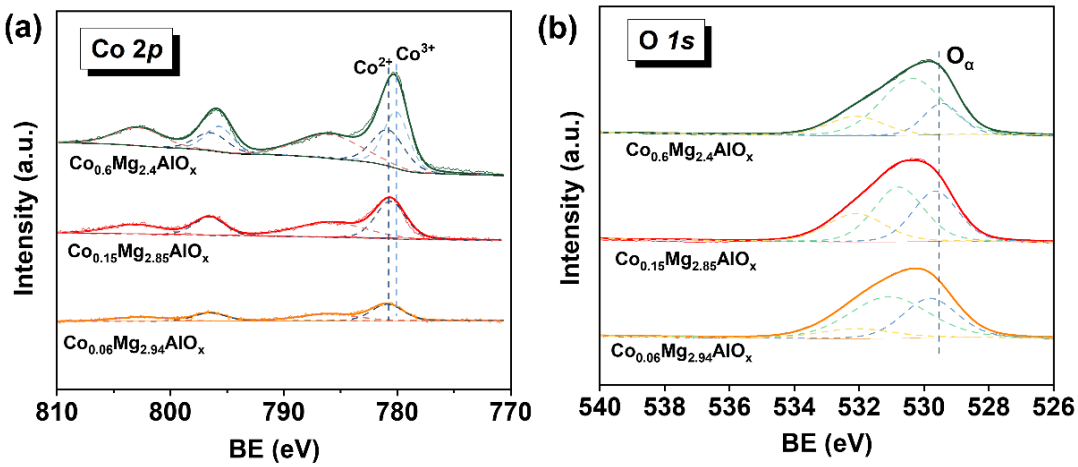

Figure S9. Co2*p* and O1*s* XP spectra for $Co_nMg_{3-n}AlO_x$

11. UV-vis DRS profiles of reduced and unreduced $Co_{0.15}Mg_{2.85}AlO_x$

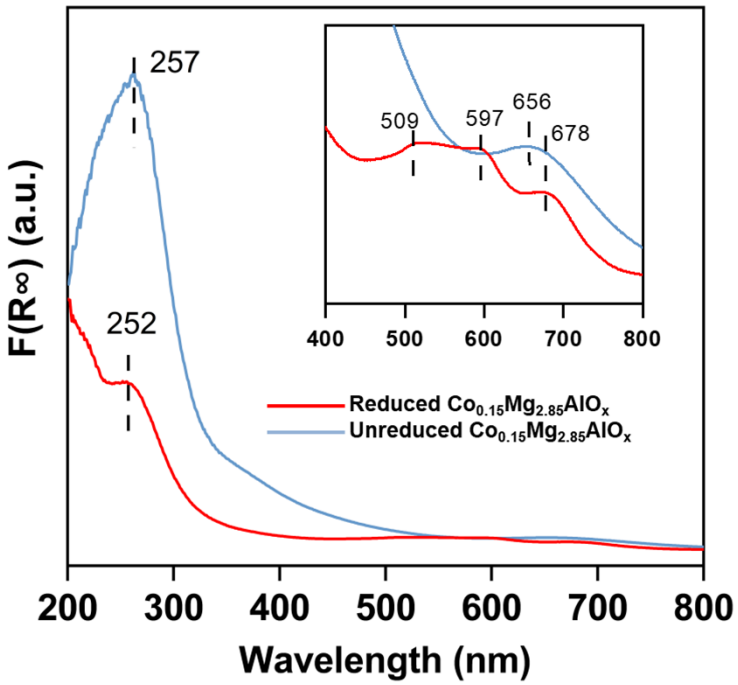

Figure S10. UV-vis DRS profiles of reduced and unreduced $Co_{0.15}Mg_{2.85}AlO_x$

12. Performance of ethanol on reduced and unreduced $Co_{0.15}Mg_{2.85}AlO_x$

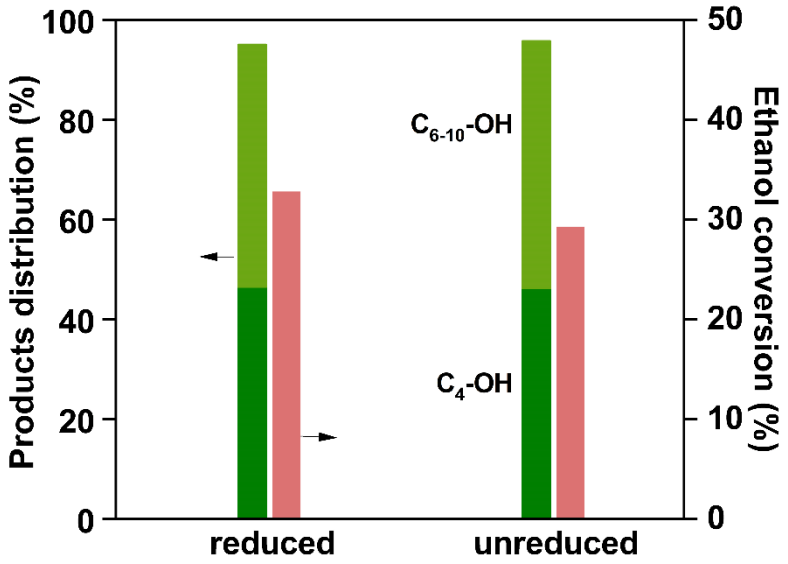

Figure S11. Comparison of catalytic performance over reduced and unreduced $Co_{0.15}Mg_{2.85}AlO_x$. Reaction conditions: 0.2 g catalysts, 5.7 kPa C_2H_5OH, WHSV=0.96 g_{C2H5OH} $g_{Cat.}$ h^{-1}, V_{total}=30 mL/min, N_2 balance.

13. Surface chemical properties of Mg_3AlO_x and $Co_nMg_{3-n}AlO_x$

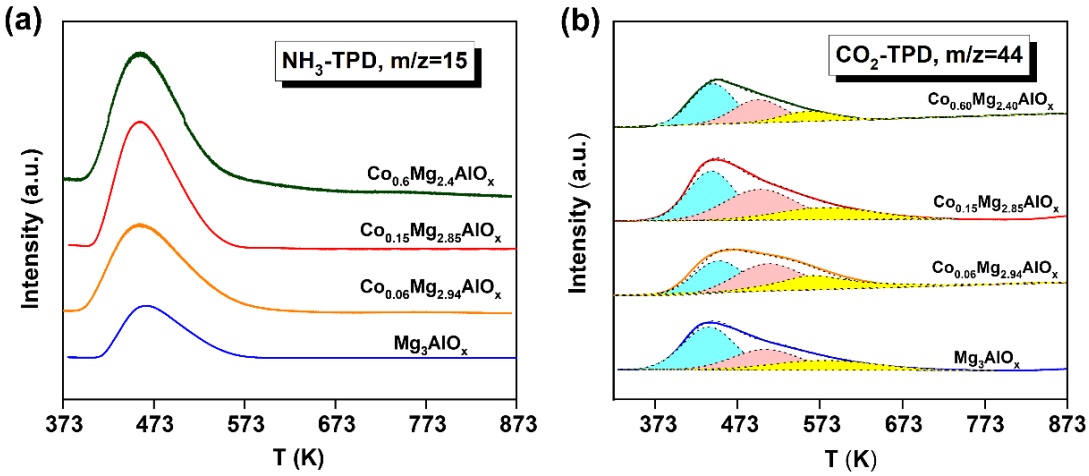

Figure S12. CO_2- (a) and NH_3-TPD-MS (b) profiles of Mg_3AlO_x and $Co_nMg_{3-n}AlO_x$.

14. The comparison of selectivity in ethanol upgrading over $Co_{0.15}Mg_{2.85}AlO_x$ and Mg_3AlO_x

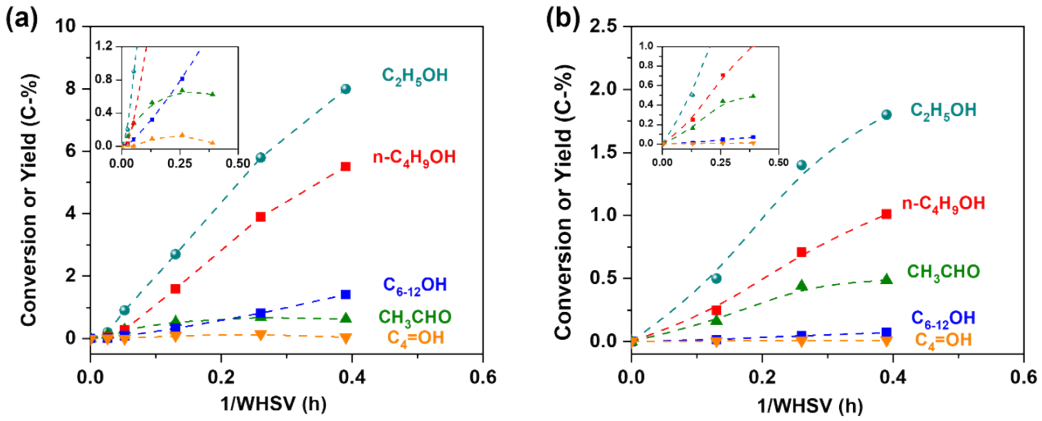

Figure S13. The comparison of selectivity in ethanol upgrading over $Co_{0.15}Mg_{2.85}AlO_x$ and Mg_3AlO_x at 523 K, showing how product yields depend on the residence time (1/WHSV). The reaction was conducted in a feed gas of 5.6 vol% C_2H_5OH/N_2 with WHSV from 0.96 to 3.85 g_{C2H5OH} g_{cat}^{-1} h^{-1}

15. Summary of catalytic activity of ethanol coupling upon different catalysts

Table S1. Summary of the catalytic data of some representative catalysts used in ethanol coupling reaction at 0.1 MPa

No.	Catalysts	T (K)	WHSV (h^{-1})	Conversion (%)	Reaction rate (mmol· $g_{Cat.}^{-1}$·h^{-1})	Selectivity (C-%)			Yield (C_{4-10}-OH)	Ref.
						n-butanol	C_{6-10}-OH	C_{4-10}-OH		
1	**$Co_{0.15}Mg_{2.85}AlO_x$**	**523**	**0.96**	**32.9**	**6.8**	**46.8**	**48.6**	**95.4**	**31.4**	**In this work**
	$Co_{030}Mg_{2.70}AlO_x$	**523**	**0.96**	**23.6**	**4.9**	**57.6**	**40.7**	**98.3**	**23.2**	
	$Co_{0.60}Mg_{2.40}AlO_x$	**523**	**0.96**	**15.7**	**3.3**	**54.8**	**43.2**	**98.0**	**15.4**	
2	Nonstoichiometric HAP	573	1.4	14.7	4.5	76.3	9.8	86.1	12.7	[1]
	HAP (Ca/P=1.62)	623	1.5	20.0	6.5	39.2	3.9	43.1	8.6	[2]
	HAP (Ca/P=1.65)	569	1.5	20.0	6.5	68.6	13.0	81.6	16.3	
	HAP (Ca/P=1.67)	571	1.5	20.0	6.5	69.8	14.5	84.3	16.9	
	HAP (Ca/P=1.67)	598	0.7	17.1	2.6	63.2	24.5	87.7	15.0	[3]
3	Mg-Al oxides (Mg/Al=3:1)	623	2.0	32.0	13.9	35.0	-	35.0	11.2	[4]

	Mg-Al oxides (Mg/Al=1:1)	623	2.0	40.0	17.3	20.0	-	20.0	8.0	
	$MgO-Al_2O_3$	573	0.05	45.0	0.5	50.0	7.0	57.0	25.7	[5]
4	4%NiMgAlO (Mg/Al=4:1)	523	3.2	18.8	13.1	55.2	31.1	86.3	16.2	[6]
		523	3.2	72.0	50.1	11.1	2.1	13.2	9.5	
		533	3.2	7.0	4.9	42.9	2.3	45.2	3.2	
5	$Ru-Mg_3Al_1$-LDO	623	3.2	29.6	24.4	70.1	12,5	82.6	24.4	[7]
	$Ru-Mg_3Al_{0.9}Ga_{0.1}$LDO	623	3.2	27.5	19.3	63.6	6.7	70.3	19.3	

16. Physical properties of the Mg_3AlO_x, $Co_{0.15}Mg_{2.85}AlO_x$ and $Co_{0.15}Mg_{2.85}AlO_x$-IM catalysts

Table S2. Physical properties of the Mg_3AlO_x, $Co_{0.15}Mg_{2.85}AlO_x$ and $Co_{0.15}Mg_{2.85}AlO_x$-IM catalysts

Catalyst	Surface area ($m^2 \cdot g^{-1}$)	Pore volume ($cm^3 \cdot g^{-1}$)	Pore size (nm)
Mg_3AlO_x	203	0.52	10.64
$Co_{0.15}Mg_{2.85}AlO_x$	175	0.54	10.54
$Co_{0.15}Mg_{2.85}AlO_x$-IM	283	0.24	3.73

17. Catalytic activity of ethanol coupling upon Mg_3AlO_x and $Co_{0.15}Mg_{2.85}AlO_x$ catalysts

Table S3. Distribution of major products over Mg_3AlO_x and $Co_{0.15}Mg_{2.85}AlO_x$ in ethanol coupling reaction [a]

Catalyst	T (K)	Conv. (%)	Selectivity (%)					Carbon balance (%)
			C_4-OH	C_6-OH	C_8-OH	C_{10}-OH	C_{4-10}-OH	
$Co_{0.15}Mg_{2.85}AlO_x$	473	8.5	78.7	14.6	1.9	0.0	95.2	99
	498	24.6	57.0	23.3	11.5	4.4	96.2	99
	523	32.9	46.8	20.8	14.8	13.0	95.4	98
	548	29.7	49.7	18.1	11.5	10.9	90.2	93
	573	29.1	46.7	14.7	7.8	13.0	82.2	90
	598	35.9	31.3	9.9	4.7	17.0	62.9	90
	623	41.4	27.9	9.3	3.6	8.4	49.2	88
Mg_3AlO_x	473	0.6	77.5	8.3	-	-	85.8	99
	498	2.7	75.5	6.8	1.2	-	83.5	99
	523	14.2	66.4	12.6	4.3	-	83.3	97
	548	23.7	57.3	15.2	9.0	-	81.5	92
	573	22.4	59.0	13.3	6.9	1.1	80.3	90
	598	29.2	52.5	13.7	6.4	1.3	73.9	85

$Co_{0.15}Mg_{2.85}AlO_x$-IM	498	10.5	78.1	17.2	1.1	-	96.4	97
	523	12.9	68.8	18.4	8.4	-	95.6	97
	548	10.9	68.3	14.5	7.9	-	90.7	94
	573	9.9	63.2	10.8	4.4	-	78.4	93
	598	12.3	51.0	8.0	2.0	-	61.0	89

[a] Reaction conditions: 200 mg catalyst, 5.7 kPa C_2H_5OH, υ_{total} = 30 mL/min, WHSV = 0.96 h^{-1}.

18. Additional References

1. T. Tsuchida, S. Sakuma, T. Takeguchi, W. Ueda, *Industrial & Engineering Chemistry Research,* 2006, **45***,* 8634-8642.

2. T. Tsuchida, J. Kubo, T. Yoshioka, S. Sakuma, T. Takeguchi, W. Ueda, *Journal of Catalysis,* 2008, **259**, 183-189.

3. C. R. Ho, S. Shylesh, A. T. Bell, *ACS Catalysis,* 2016, **6**, 939-948.

4. D. L. Carvalho, R. R. de Avillez, M. T. Rodrigues, L. E. P. Borges, L. G. Appel, *Applied Catalysis A: General,* 2012, **415-416**, 96-100.

5. K. K. Ramasamy, M. Gray, H. Job, D. Santosa, X. S. Li, A. Devaraj, A. Karkamkar, Y. Wang, *Topics.in Catalysis,* 2016, **59**, 46-54.

6. J. Pang, M. Zheng, L. He, L. Li, X. Pan, A. Wang, X. Wang, T. Zhang, *Journal of Catalysis*, 2016, **344**, 184-193.

7. Yuan B , Zhang J , An Z , et al. Atomic Ru Catalysis for Ethanol Coupling to C4+ Alcohols. *Applied Catalysis B: Environmental,* 2022, **309,**121271